Binding and Reactivity of *Candida albicans* Estrogen Binding Protein with Steroid and Other Substrates†

James Buckman and Susan M. Miller*

Department of Pharmaceutical Chemistry, University of California, San Francisco, California 94143-0446

Received May 13, 1998; Revised Manuscript Received July 24, 1998

ABSTRACT: In this report recombinant estrogen binding protein (EBP1), isolated originally from *Candida albicans* as a result of its high affinity for 17β-estradiol, has been purified extensively using a modified affinity purification scheme originally developed for a homolog of EBP1, old yellow enzyme (OYE). It is shown that like OYE, the protein binds a variety of compounds with a phenolic structure, including 17β-estradiol, and compounds with an α,β-unsaturated keto or aldehyde structure. In addition, EBP1 exhibits an NADPH oxidoreductase activity, transferring electrons from NADPH to all α,β-unsaturated ketones and aldehydes tested via the tightly bound FMN cofactor. Analysis of the steady-state kinetics of these reactions indicate a tetra uni ping-pong mechanism. Inhibition of the steady-state reaction by 17β-estradiol gives a $K_i = 10 \pm 2$ nM, and indicates exclusive binding of this steroid to the enzyme in its oxidized state. In contrast, 19-nortestosterone binds to both oxidized and reduced forms of the enzyme with dissociation constants of 600 ± 100 and 650 ± 90 nM, respectively. EBP1 also catalyzes a disproportionation reaction with certain compounds, in which two molecules of a cylic α,β-unsaturated ketone, including the steroid 19-nortestosterone, are individually aromatized and reduced to the corresponding saturated ketone. Despite the extensive similarity in sequence and enzymic activity, notable differences between EBP1 and the OYE family of proteins exist with regard to the binding behavior and reactivity with the two steroids tested here, estradiol and 19-nortestosterone.

Several studies suggest that *Candida albicans* undergoes changes in its morphology and growth rate in response to estrogens supplied in the growth medium (*1*−*3*). Epidemiological surveys and studies of virulence in animal models have suggested that this characteristic contributes to the pathogenicity of the fungus, perhaps enabling the organism to more successfully evade the immune system of the host (*4*). The estrogen binding protein (EBP1)[1] was isolated from *C. albicans* as a result of its high, specific affinity for 17β-estradiol (*5*) and represents the only significant estrogen binding activity identified in the organism thus far.[2] Thus, it is conceivable that EBP1 acts as a mediator in processes leading to the gross physiological changes seen upon exposure to estrogens and, as such, may be an important element in studying this phenomenon and its effect on virulence.

Sequence analysis of EBP1 indicates that it is not similar to other members of the steroid receptor superfamily, but instead displays ~46% identity to the various isozymes of the long-studied NADPH oxidoreductase of brewer's bottom yeast, old yellow enzyme (OYE) (*6*). OYE was the first identified flavoprotein (*7*) and has served as a paradigm in the study of its redox-active flavin mononucleotide (FMN) cofactor that gives it its distinct yellow color. Despite extensive study of the binding and redox behavior, the physiological substrates and role of the several OYE's that have now been sequenced (*8*) are not known. Other homologs of OYE have been identified in several organisms (*9*−*11*), both eukaryotic and prokaryotic. The recent cloning and sequencing of 12-oxophytodienoate (OPDA) reductase from the plant species *Arabidopsis thaliana* (*12*), revealed 37.5−39.1% amino acid sequence identity to the OYE isozymes, and 32.4% identity with EBP1. This protein catalyzes the reduction of an intermediate in the octadecanoid signaling pathway in *Arabidopsis*, and is the first member of the OYE homology family for which an endogenous substrate has been identified. Furthermore, the indication that the homolog OPDA reductase is involved in a pathway important for intercellular communication and defense provides a new lead for study of the role of EBP1 and the effect of estrogens on *C. albicans*.

† This work was supported by a Faculty Development Award and Individual Investigator Grant from the UCSF Academic Senate (S.M.M.). J.B. received a stipend from an NIH Pharmaceutical Sciences Training Grant GM07175, and fellowships from the American Foundation for Pharmaceutical Education and Achievement Rewards for College Scientists during the course of this work.

* To whom correspondence should be addressed. Telephone: 415-476-7155. Fax: 415-476-0688. E-mail: smiller@cgl.ucsf.edu.

[1] Abbreviations: CHES, 2-[*N*-cyclohexylamino]ethane sulfonic acid; CHX, 2-cyclohexenone; EBP1, estrogen binding protein (see footnote 2); E_{ox}, oxidized EBP1; E_{red}, reduced EBP1; $E_{sq}^{\bullet}$, semiquinone form of EBP1; EDTA, ethylenediaminetetraacetic acid; estradiol, 17β-estradiol; FMN, flavin mononucleotide; HXL or hexenal, *trans*-2-hexenal; MES, 2-[*N*-morpholino]ethanesulfonic acid; OPDA, 12-oxophytodienoate; PCR, polymerase chain reaction; RP-HPLC, reverse-phase high-performance liquid chromatography; SDS−PAGE, sodium dodecyl sulfate−polyacrylamide gel electrophoresis; LB, Luria-Bertani.

[2] Southern blots of *Candida albicans* DNA using sequence probes from cloned gene for EBP1 suggest the presence of at least one other similar sequence in the genome; hence, this protein was designated EBP1 (*6*).

S0006-2960(98)01106-4 CCC: $15.00
Published on Web 09/12/1998

As with the OYE's, the physiological function of EBP1 has not yet been identified. It has been demonstrated that EBP1 possesses steroid-binding activity, and preliminary studies suggest it has an NADPH oxidase activity that is inhibited by estradiol (*6*). Given the possibility that EBP1 functions in some way to communicate the hormonal environment of its host and thus mediate a response to that environment, it is important to understand the role of EBP1 and its enzymatic activity and to more carefully examine the impact that steroid binding has upon it.

Using an adaptation of a purification regime developed originally for isolation of OYE (*13*), we have obtained highly purified native and recombinant EBP1. Described here is the characterization of the redox activity with NADPH and other compounds, steroid reactivity and inhibition behavior, and the ligand-binding properties of this enzyme. The similarities and differences in these properties between OYE and EBP1 and their implications are discussed.

MATERIALS AND METHODS

Unless indicated otherwise, all reagents used were the highest grade possible and obtained from Sigma Chemical. *C. albicans* strain 422 and *Escherichia coli* containing a pMAL plasmid in which the EBP1 gene sequence was fused in frame behind that encoding a maltose-binding domain were generously provided to us by Drs. Peter Malloy and David Feldman (Stanford).

Purification of EBP1. EBP1 was purified using a modified protocol similar to that described previously for the purification of OYE, which exploits the ability of these proteins to bind phenolic ligands (*13*). Briefly, *p*-hydroxybenzoate was coupled to commercially available ω-aminohexyl agarose using 1-ethyl-3-(3-diethylaminopropyl)carbodiimide to yield a phenolic (i.e, *p*-hydroxybenzamide) affinity resin. *E. coli* containing the pMAL fusion plasmid were grown in LB media at 37 °C, and the expression of the fusion protein was induced using the protocol suggested by the manufacturer (New England Biolabs). After 4 h of induction, cells were harvested, resuspended in 0.1 M Tris-HCl buffer, pH 8.3, 10 mM EDTA, and lysed by sonication. Inclusion of Bowman-Birk trypsin−chymotrypsin inhibitor (Sigma) in the lysis buffer did not result in significant improvement in the final yield of active enzyme. The supernatant was passed through a 500 mL column containing 100 mL of the derivatized agarose described above, during which a dark green band accumulated at the top of the column that indicated binding of EBP1. After washing with ~1.2 L of lysis buffer, the fusion protein was eluted with ~200 mL of the same buffer containing 50 mM phenol. The protein was concentrated in a Centriprep-30 concentrator (Amicon), resuspended in 20 mM Tris-HCl, pH 7.5, 0.1 M KCl, and passed through a column containing 500 mL of desalting gel, BIO-GEL P-6 DG (BIORAD) that had been pre-equilibrated with the same buffer. In the time required for the protein to reach the bottom of the column, the remaining phenol dissociated and was retained on the column so that it was quantitatively removed, as evidenced by the UV−vis absorption spectrum of the eluted EBP1 (see Results). NaCl and $CaCl_2$ were added to final concentrations of 0.1 M and 2 mM, respectively, followed by addition of Factor Xa (New England Biolabs) (0.5 mg/mg of fusion protein as determined by UV−vis absorbance, using a value for the extinction coefficient of the noncovalently bound FMN cofactor at 466 nm of 10 750 M^{-1} cm^{-1} as determined previously (*14*)) to cleave the maltose-binding domain from EBP1. After incubation at room temperature for 8 h, the reaction mix was passed through a 100 mL column containing 50 mL of Cibacron Blue affinity purification resin (Amicon Dye Matrex), which binds EBP1, but not the maltose-binding domain, Factor Xa, or any other proteins isolated in the first chromatographic step. EBP1 was eluted by addition of 20 mM Tris-HCl, pH 7.5, 2 M KCl, concentrated by centrifugation in a Centriprep-30 cell, desalted by passage through Sephadex G-25, filtered, and stored at −20 °C. Purity of protein isolated in this manner routinely exceeds 95%, as determined by either silver or Coomassie staining of the material after SDS−PAGE (data not shown). This protocol yields far greater quantities of pure EBP1 than the manufacturer's scheme, which makes use of the maltose-binding domain in isolating the fusion protein. Therefore, to eliminate the need for Factor Xa proteolysis, we subcloned the gene encoding EBP1 into a pET expression vector (Stratagene).

Subcloning EBP1 into the pET Expression Vector. Primers complementary to the 5′ and 3′ sequence were designed to amplify the EBP1 gene using PCR. The 5′ primer, CTCGGAGCATATGACTATTGAATCAACTA, included 10 additional nucleotides to generate an *Nde*I restriction endonuclease site (underlined), and the 3′ primer, CCGGATCCCTATGCCAATGGTTTACC, included 8 additional nucleotides to generate a *Bam*HI site (underlined) on the 5′- and 3′-ends of the amplified product, respectively. The pMAL plasmid containing the EBP1 gene was isolated from *E. coli* cells using the Wizard Plus Miniprep DNA purification system (Promega) and incubated with the primers. The EBP1 sequence was amplified using the GeneAmp PCR reagent kit and a thermal cycler (Perkin-Elmer) and was subsequently purified using standard techniques (*15*). To facilitate subsequent digestion with the restriction endonucleases, the amplified product was incubated with the p-GEM-T vector (Promega) and T4 DNA ligase, and was then used to transform competent *E. coli* DH5α cells (Gibco BRL). Transformants were isolated and those containing the proper insert were detected by separate restriction digests with first *Nde*I, then *Bam*HI (New England Biolabs), using reagents supplied with each enzyme, followed by agarose gel electrophoresis to identify fragments of the appropriate length. The EBP1 sequence, now containing the appropriate 5′ and 3′ modifications for ligation into the multicloning site of the pET-3a vector in the appropriate orientation, was purified from the agarose gel as above. The insert and vector were digested with *Nde*I and *Bam*HI and incubated overnight with T4 DNA ligase at 16 °C, and the ligation mixture was used to transform competent *E. coli* BL21(DE3) cells. Two colonies were isolated that contained the correct construct, as identified by restriction digestion and agarose gel electrophoresis to identify fragments of appropriate length. Large-scale growth of these transformants yielded active protein, which was indistinguishable from that isolated using the pMAL system, on the basis of both kinetic analysis and the UV−vis absorbance properties, but was of higher purity (~98%), as determined by SDS−PAGE. Purification of protein expressed from this construct was the same as

Scheme 1

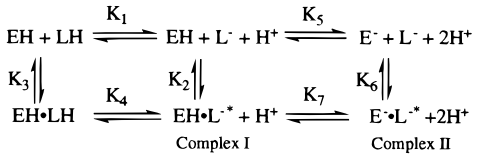

described above, except that in this case, protein eluted from the P6-DG column was applied directly to the Cibacron Blue column. Native enzyme was isolated by the same procedure from *C. albicans* strain 422 grown in Sabouraud's dextrose broth (Difco) overnight at 30 °C.

Ligand-Binding Titrations. Unless otherwise indicated, titrations were performed in a buffer system consisting of 100 mM MES, 51 mM *N*-ethylmorpholine, and 51 mM diethanolamine, which maintains nearly constant ionic strength across the pH range 5−10 (*16*). Typically, a stock solution of enzyme in 1 mM potassium phosphate buffer, pH 7.5, was diluted 10-fold into the buffer system above, which had been adjusted to the appropriate pH with either HCl or KOH. 17β-Estradiol (estradiol) (Steraloids, Inc.) and 19-nortestosterone were dissolved in ethanol such that the final concentration of ethanol at the endpoint of the titrations was less than 5%. This amount of ethanol has no effect on the enzyme, as determined by both kinetic and spectroscopic measurements. Stock solutions of phenol were dissolved in titration buffer. Spectra were recorded using a Shimadzu UV-2101PC double-beam absorbance spectrophotometer, and resulting data were analyzed using SPECFIT (Spectrum Software Associates, Chapel Hill, NC), a program that employs a singular value decomposition routine, global least-squares fitting, and factor analysis of the entire set of spectral data to yield values for kinetic or equilibrium binding constants for a specified model. Extinction coefficients at 578 nm for the E_{ox}•phenol complex were obtained at different pH values after addition of a sufficient amount of a concentrated stock solution of phenol to saturate the enzyme. Using the curve-fitting routine in KaleidaGraph (Abelbeck Software), the pH dependence of ϵ_{app} at 578 nm was fit to eq 1, which describes the proportion of a diprotic acid existing in both the mono- and dibasic forms as a function of pH:

$$\epsilon_{app} = \frac{\epsilon_1 K_4[H^+] + \epsilon_2 K_4 K_7}{K_4[H^+] + [H^+]^2 + K_4 K_7} \quad (1)$$

where K_4 and K_7 represent the acid dissociation constants, and ϵ_1 and ϵ_2 are the extinction coefficients at 578 nm for the pure species EH•L^- and E^-•L^-, respectively (based on the data, the extinction coefficient for the fully protonated complex is negligible; see Results and Scheme 1). Though the value for K_4 resulting from this analysis agreed well with that determined from the analysis of the binding data described below, the value for K_7 could be varied widely with little effect on the correlation with the data. The fit shown in the inset of Figure 2A was obtained, therefore, by constraining the value of K_7 to that determined in the analysis that follows.

Apparent dissociation constants, obtained using SPECFIT, are a complex function of the various equilibria described in Scheme 1, from which the analytical solution can be derived, as described by Dixon (*17*). The data were fit to eq 2 using KaleidaGraph:

$$-\log K_{d(app)} = \log\left(1 + \frac{K_4}{[H^+]} + \frac{K_4 K_7}{[H^+]^2}\right) - \log\left(1 + \frac{K_1}{[H^+]}\right) - \log\left(1 + \frac{K_5}{[H^+]}\right) - \log K_3 \quad (2)$$

where K_1, K_4, K_5, and K_7 are acid dissociation constants, and K_3 is the dissociation constant for the fully protonated enzyme•ligand complex, as indicated in Scheme 1.

Steady-State Kinetics. Steady-state rates were determined in 0.1 M potassium phosphate buffer, pH 7.5, at 25 °C, by systematic variation of the concentration of both substrates to yield a matrix of data points. Substrate stock solutions were prepared in 0.1 M potassium phosphate buffer, pH 7.5, except for the pyridine nucleotide cofactor, which was prepared in 20 mM un-neutralized Tris. At low NADPH concentrations, rates were determined using 1 nM EBP1 by following the decay of NADPH fluorescence ($\lambda_{ex} = 340$ nm, $\lambda_{em} = 454$ nm) using a Perkin-Elmer luminescence spectrometer LS50B. At high NADPH concentrations, rates were obtained with 10 nM EBP1 by monitoring the decrease in absorbance at 340 nm using a Cary 118. One concentration of NADPH was examined by both methods in order to normalize and combine the data. Data obtained from the fluorescence assay exhibited greater error compared with the absorbance data, especially with the lower NADPH concentrations, in the presence of inhibitors.

All kinetic data, including those obtained using low concentrations of 2-cyclohexenone ($\leq 56\ \mu$M), were analyzed using the enzyme kinetics analysis package, KinetAsyst II (IntelliKinetics, State College, PA). This program allows a set of initial velocity data measured as a function of the concentration of substrate(s) (and inhibitor, where appropriate) to be evaluated in the context of several possible kinetic models. The kinetic model assigned in each case was that which gave the best fit to the data with the smallest global least-squares deviation.

The lines in the double-reciprocal plots of Figures 4 and 5 were generated by substituting the kinetic constants so obtained into eq 3, which describes the dependence of the initial velocity on substrate concentrations in a ping pong system:

$$\frac{1}{k_{app}} = \frac{K_{mA}}{k_{cat}}\frac{1}{[A]} + \frac{K_{mB}}{k_{cat}}\frac{1}{[B]} + \frac{1}{k_{cat}} \quad (3)$$

where A represents NADPH, and B represents either *trans*-2-hexenal or 2-cyclohexenone.

The data obtained with 2-cyclohexenone as substrate at high concentrations ($>56\ \mu$M) indicated significant substrate inhibition (see Figure 4 and corresponding discussion below). Therefore, these were fit to eq 4 for competitive (substrate) inhibition in a ping pong system (*18*) using KaleidaGraph to obtain a value for the dissociation constant for the "dead-end" complex of that compound with oxidized enzyme, K_i:

$$\frac{1}{k_{app}} = \frac{K_{mA}}{k_{cat}}\frac{1}{[A]}\left(1 + \frac{[I]}{K_i}\right) + \frac{K_{mB}}{k_{cat}}\frac{1}{[B]} + \frac{1}{k_{cat}} \quad (4)$$

where A is NADPH, and in this case, both I and B represent 2-cyclohexenone.

Analysis with KinetAsyst II of the inhibition of steady-state turnover by estradiol, varying the concentration of one substrate while keeping the other constant, indicated that estradiol was competitive with respect to NADPH and uncompetitive with respect to *trans*-2-hexenal. The values obtained for the dissociation constant for the E_{ox}·estradiol complex, K_i, from each analysis agree well, and the lines in Figure 6A,B were generated by substitution of the average value into eq 4, where A is NADPH, B is *trans*-2-hexenal, and I is estradiol.

Examination of the velocity data in the presence of 19-nortestosterone revealed that this compound displays mixed inhibition, and the constants obtained from the analysis with KinetAsyst II were substituted into eq 5, which describes mixed inhibition in a ping pong system to generate the lines in Figure 7A,B:

$$\frac{1}{k_{app}} = \frac{K_{mA}}{k_{cat}}\frac{1}{[A]}\left(1+\frac{[I]}{K_i}\right) + \frac{K_{mB}}{k_{cat}}\frac{1}{[B]}\left(1+\frac{[I]}{K_i'}\right) + \frac{1}{k_{cat}} \quad (5)$$

where A is NADPH, B is *trans*-2-hexenal, I is 19-nortestosterone, and K_i and K_i' are the dissociation constants for the complex of 19-nortestosterone with oxidized and reduced enzyme, respectively.

Anaerobic Experiments. Anaerobic experiments described here were performed using specially designed cuvettes similar to those previously described (*19*). Samples were made anaerobic by successive cycles of evacuation and re-equilibration with oxygen-scrubbed argon. To examine reactions with oxidized enzyme, 2-cyclohexenone or 19-nortestosterone was added to a sidearm in the cuvette before anaerobiosis. Spectra were recorded prior to and immediately after tipping the contents of the sidearm into the enzyme solution and at successive time points, as indicated in the figure legends. To examine the reaction of 19-nortestosterone with the reduced enzyme, the cuvette was treated as above, and the anaerobic oxidized enzyme was reduced by titration with sodium dithionite before tipping in the steroid. After anaerobic incubation of either oxidized or reduced enzyme with 19-nortestosterone for more than 24 h, the reaction mix (total volume of ~20 mL) was extracted with ~5 mL of chloroform and centrifuged to separate the phases. The organic phase was subsequently transferred to a clean glass vial, and the chloroform was evaporated under a stream of nitrogen. The dried material was then stored at −20 °C and analyzed by high-resolution electron impact mass spectrotrometry using a VG70 spectrometer at the UCSF Mass Spectrometry Facility (A. L. Burlingame, Director), which is supported by the Biomedical Research Technology Program of the National Center for Research Resources, NIH NCRR BRTP RR04112 and RR01614.

Determination of Redox Potential. The midpoint reduction potential of the EBP1-bound FMN cofactor was determined by reducing the protein (31 μM) anaerobically with dithionite in the presence of an approximately equimolar amount of the redox active dye, phenosafranine. A small amount of methyl viologen (final concentration ~ 2 μM) was added to equilibrate electrons within the system. The midpoint potential for the protein was obtained from a plot of the log of the ratio of oxidized to reduced protein versus that of the dye, using a value of −252 mV (*20*) for the midpoint potential of phenosafranine (data not shown).

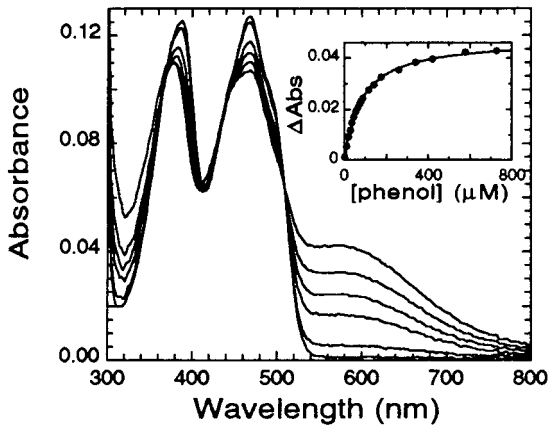

FIGURE 1: UV−Vis absorption spectra that accompany addition of phenol to EBP1. Spectra with increasing absorbance at 600 nm were obtained after addition of phenol with a final concentration of 0, 8.8, 44, 87, 172, and 576 μM to 11.8 μM EBP1 at pH 7.3 as described in text. Inset: Increase in absorbance at 578 nm as a function of ligand concentration with fit using SPECFIT that yields a $K_{d(app)} = 80$ μM.

RESULTS

Ligand Binding. Previous experiments with radiolabeled steroid established the estrogen-binding activity in EBP1 (*6*); however, the binding site cannot be identified by this method. A distinctive property of the EBP1 homolog, OYE, is its proclivity to bind various phenolic ligands in their deprotonated state adjacent to the flavin cofactor. Formation of such complexes leads to changes in the optical absorption spectrum, including shifts in the position and shape of the major flavin bands, and the appearance of a new, long-wavelength absorption band (*21*). Various lines of evidence indicate that these changes arise from a charge-transfer interaction between the phenoxide ligand and the oxidized FMN cofactor (*22*, *23*). Thus, we performed titrations of EBP1 with both phenol and estradiol, which contains a phenolic A ring (see Figure 3, inset), to examine the effects these compounds have on the flavin absorbance and to determine whether they bind adjacent to the flavin in the presumed active site of EBP1.

As shown in Figure 1, titration of EBP1 with phenol at pH 7.3 results in broadening of the main flavin bands centered at 385 and 466 nm in the unliganded protein, a shift of the λ_{max} of these bands to shorter wavelengths, and the appearance of a long-wavelength absorption band with a maximum at 578 nm. The changes in the absorption spectrum, especially the intensity of the long-wavelength band are pH-dependent (Figure 2A), as expected for a charge-transfer interaction between a deprotonated ligand and the active site flavin. To determine the pK_a of the bound ligand and whether additional residues on the enzyme affect the enzyme−ligand interaction, we examined the behavior of both the extinction coefficient of the charge-transfer absorption band as well as the binding affinity over a broad pH range (Figure 2A,B). As shown in Figure 2B (dashed line), the pH behavior of the binding affinity cannot be described

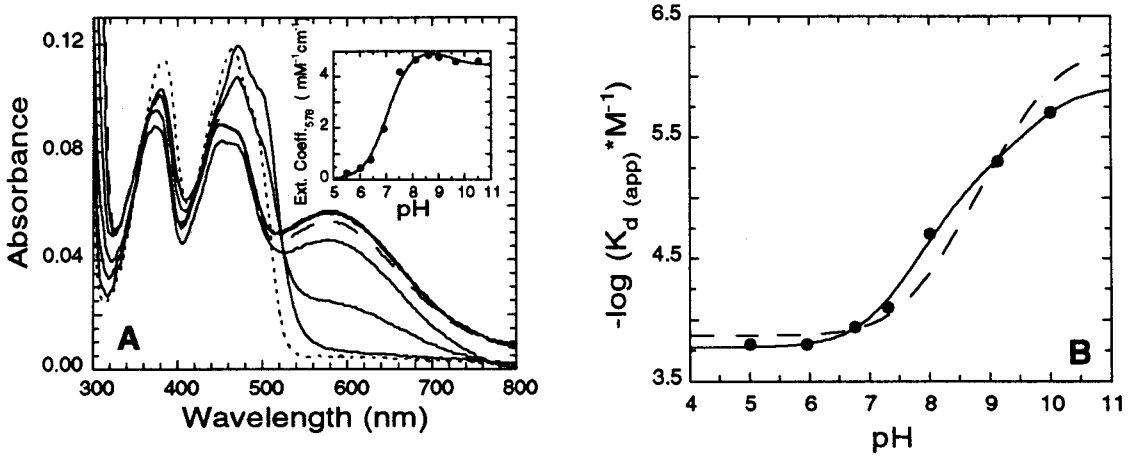

FIGURE 2: Dependence of binding affinity and charge-transfer intensity on pH. (A) Solid lines with increasing absorbance at 578 nm are spectra collected after adding a saturating concentration ($\geq 8K_d$) of phenol to 11.8 μM EBP1 at pH 5.5, 6.9, 7.5, 8.6, and 9.6, respectively. Absorbance of the complex at 578 nm peaks at pH ~10 (see inset), after which it begins to decrease again, as shown by the dashed line spectrum collected at pH 10.5. For reference, the spectrum of the unliganded enzyme at pH 5.5 is included (dotted line). Inset: Extinction coefficients obtained as described. Solid line represents a fit to the data using the value of K_7 determined in (B) and yields a value for K_4 of $(9 \pm 1) \times 10^{-8}$ M and extinction coefficients for complexes I and II at 578 nm of 5100 ± 200 and 4400 ± 200 M^{-1} cm^{-1}, respectively. (B) Dissociation constants were determined as described in text. Dashed line indicates a fit to the data with a model assuming only the ionization of phenol is relevant to binding affinity. Solid line represents fit including all species shown in Scheme 1 and yields the following values for equilibrium constants: $K_3 = 1.7 \pm 0.2 \times 10^{-4}$ M, $K_4 = 8 \pm 2 \times 10^{-8}$ M, $K_5 = 2 \pm 1 \times 10^{-9}$ M, and $K_7 = 4 \pm 3 \times 10^{-10}$ M.

adequately by a model in which only deprotonation of phenol is included (left box of Scheme 1); a fit of the data with this model proscribes a solution pK_a of 9.1 for phenol, nearly a full pH unit below its reported value (*24*). This result is also apparent from careful examination of the full spectra of the complexed enzyme as a function of pH, Figure 2A, where the isosbestics observed at low pH (ca. 767 and 525 nm) are lost at higher pH values. Including a deprotonation of the protein in the model (full Scheme 1) results in a good correlation with the experimental data and the reported pK_a of 10.0 for phenol free in solution (Figure 2B, solid line). Analysis of the binding data is consistent with the interpretation of the extinction coefficient data (Figure 2A, inset), and indicates that the pK_a of phenol is lowered almost three units from 10.0 to ~7.3 upon binding to EBP1, and that the pK_a of a group on the free protein is raised from ~8.6 to 9.4 in the complex. The model in Scheme 1 describes the various deprotonations and complexes that account for these results, and assumes that only those complexes in which the ligand is deprotonated (marked by asterisks) are responsible for charge-transfer absorbance, a conclusion well supported by data from titrations at low pH (see Figure 2A, pH 5.5). A similar model was developed from the results of studies on the pH dependence of *p*-chlorophenol binding to OYE; however, in that case neither the high nor the low pH plateaus were observed, indicating that the two pK_a's of the bound species were shifted further outside the range of the experiments (*23*).

Analysis of the data using eq 2 yields all of the acid dissociation constants (K_1, K_5, K_4, and K_7) as well as the equilibrium constant describing dissociation of the fully protonated complex ($K_3 = (1.7 \pm 0.2) \times 10^{-4}$ M). The remaining dissociation constants are obtained by completing the thermodynamic cycle:

$$K_2 = K_1K_3/K_4 = (1 \times 10^{-10}\ \text{M})(1.7 \pm 0.2 \times 10^{-4}\ \text{M})/(8 \pm 2 \times 10^{-8}\ \text{M}) \approx 2 \times 10^{-7}\ \text{M}$$

$$K_6 = K_2K_5/K_7 = (2 \pm 0.6 \times 10^{-7}\ \text{M})(2 \pm 1 \times 10^{-9}\ \text{M})/(4 \pm 3 \times 10^{-10}\ \text{M}) \approx 1 \times 10^{-6}\ \text{M}$$

Comparison of K_3, K_2, and K_6 indicates that the ionization of phenol is extremely important for both binding and charge-transfer development, resulting in an ~850-fold increase in the tightness of binding over the fully protonated species and an increase in the extinction coefficient by ~5100 M^{-1} cm^{-1}. The deprotonation of the protein, on the other hand, has more modest effects, weakening binding of the enzyme·phenoxide complex only ~6-fold, and decreasing charge-transfer intensity by ~15%. Further work is necessary to determine the identity of the group on the protein responsible for this effect.

In contrast to results with OYE (*25*), titration of EBP1 with estradiol at pH 7.3 results in changes of the flavin absorbance that are quite different from those that occur upon addition of phenol at the same pH (Figure 3). The low-intensity long-wavelength absorbance that develops is broad, much like that which develops in the titration with phenol at lower pH (cf. Figure 2A), where the spectrum reflects a mixture of phenol and phenoxide complexes. Saturation with estradiol at higher pH (e.g., 9.3) results in a spectrum that resembles that of the E_{ox}·phenoxide spectrum at pH 8−9 (compare Figure 3, dashed line, with Figure 2A) but with a λ_{max} = 640 nm for the charge-transfer transition. This implies that these ligands bind similarly to the enzyme, and although the full pH dependence was not characterized, this and other data suggest that the pK_a for bound estradiol is somewhat higher than that for bound phenol. The dependence of the dissociation constant for estradiol on pH was not measured because binding was stoichiometric even at pH 7.3, and thus too tight to be determined reliably in this manner. The spectra obtained during the titration with estradiol were stable, and there was no indication of a chemical conversion of estradiol by EBP1.

Midpoint Potential Determination. Although the overall spectral changes associated with binding of phenol are similar

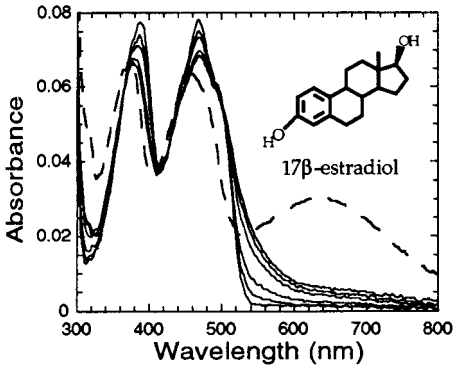

FIGURE 3: UV−Vis absorption spectra that accompany titration of EBP1 with estradiol. Solid curves with increasing absorbance at 550 nm are spectra obtained after addition of 0, 0.14, 0.28, 0.64, 0.78, and 1 equivalent of estradiol to 7.2 μM EBP1 in 0.1 M phosphate buffer, pH 7.3. Dashed line is final spectrum resulting from saturation of EBP1 with estradiol in 0.1 M CHES buffer, pH 9.3. Spectra are normalized to starting concentration of enzyme in each experiment, as determined by A_{466}. Binding is too tight to determine the K_d accurately from these experiments.

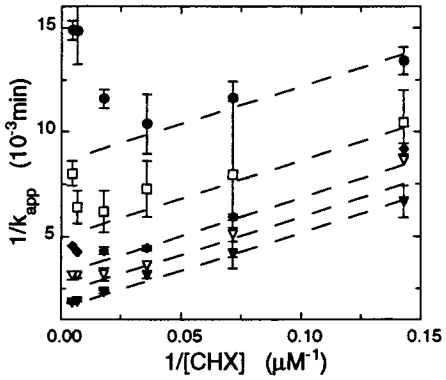

FIGURE 4: Double-reciprocal plot of steady-state velocity data with NADPH and 2-cyclohexenone as substrates: (—●—) 0.25 μM, (—□—) 0.5 μM, (—◆—) 1 μM, (—▽—) 2 μM, and (—▼—) 15 μM NADPH. Curves were generated from kinetic constants obtained by analysis of data at [CHX] $\leq$ 56 μM, as described, yielding $K_{mNADPH} = 1.3 \pm 0.2$ μM, $K_{mCHX} = 26 \pm 5$ μM, and $k_{cat} = 710 \pm 30$ min^{-1}.

Scheme 2

$$E_{ox} + NADPH \rightleftharpoons E_{ox} \cdot NADPH \rightleftharpoons E_{red} \cdot NADP^+ \rightleftharpoons E_{red} + NADP^+$$

$$E_{red} + \text{⬡=O} \rightleftharpoons E_{red} \cdot \text{⬡=O} \rightleftharpoons E_{ox} \cdot \text{⬡=O} \rightleftharpoons E_{ox} + \text{⬡=O}$$

in EBP1 and OYE, they differ in the position of the λ_{max} for the charge-transfer absorbance (578 nm for EBP1 versus 610 nm for OYE) (*23*). A possible explanation for this difference comes from a study of the variation of the position of the charge-transfer absorbance in OYE substituted with native and artificial flavins of varied redox potential (*22*). In that study, the energy of the charge-transfer band was shown to be dependent on the ionization potential of the charge-transfer donor (the phenol) and the electron affinity of the acceptor (represented by the one-electron reduction potential of the oxidized flavin). Derivatized flavins of lower potential are more difficult to reduce and, therefore, less able to accept electron density from the donor. As a result, the position of the charge-transfer band with protein reconstituted with these lower potential flavins occurs at higher energy (shorter wavelength). On this basis, we postulated that the difference in the position of the charge-transfer bands in EBP1 versus OYE might be the reflection of a difference in the redox potential of the FMN cofactor bound to each enzyme. Indeed, the midpoint potential of -246 ± 1 mV measured here for EBP1 is 16 mV more negative than that reported for OYE (*22*). It should be noted that this is the two-electron potential for reduction of E_{ox} to E_{red}. Unlike OYE, the one-electron reduced semiquinone species, $E_{sq}^{\bullet}$, is *not* thermodynamically stabilized in EBP1 (unpublished observation, see discussion). This indicates that the one-electron potential for reduction of E_{ox} to $E_{sq}^{\bullet}$ is lower than the two-electron potential in EBP1, in contrast to OYE, where the one-electron potential is actually higher than the two-electron potential (*22*). Given that the two-electron potential for EBP1 is 16 mV lower than that for OYE, the one-electron potential must be substantially lower than that for OYE. This is further consistent with the shorter wavelength for the charge-transfer band in EBP1, since the correlation observed by Stewart and Massey (*22*) was with the one-electron potential for formation of $E_{sq}^{\bullet}$.

Steady-State NADPH Oxidoreductase Activity. The spectral properties of the estradiol complex with oxidized enzyme strongly suggest that this steroid does indeed bind adjacent to the flavin. As this is very likely the active site of the enzyme, estradiol is expected to be a potent inhibitor of its activity. To study inhibition by estradiol, we first needed to develop an appropriate assay of enzymatic activity. Previous assays of crude cytosolic preparations of EBP1 suggested that, like OYE, it exhibits an NADPH oxidase activity that is stimulated by 2-cyclohexenone and inhibited by estradiol (*6*). Using purified native and recombinant protein, we have verified that the enzyme catalyzes the two-electron reduction of 2-cyclohexenone to cyclohexanone using reduction equivalents from NADPH, and have examined the steady-state kinetic mechanism of the reaction. Analysis of steady-state turnover, varying concentrations of both substrates, reveals a complex dependence on the concentration of 2-cyclohexenone (Figure 4). At low concentrations of 2-cyclohexenone, the data asymptotically approach the parallel lines associated with ping pong kinetics, in which each substrate binds and reacts with the enzyme independently in a separate half-reaction (Scheme 2). This mechanism is further supported by anaerobic titrations in which NADPH reduces the flavin in the absence of an electron acceptor, and enzyme reduced with dithionite is stoichiometrically reoxidized by 2-cyclohexenone (unpublished observations). However, at higher concentrations of 2-cyclohexenone, the data deviate from the expected value for this simple system. In particular, the velocity is considerably lower than expected at low concentrations of NADPH, indicating a competitive relationship with the "first" substrate for the enzyme, that is, 2-cyclohexenone also binds to the oxidized form of the enzyme and prevents electron transfer from NADPH (see below and Scheme 3). The inhibition constant obtained from analysis of these data is 300 ± 100 μM and represents the dissociation constant for the complex of oxidized enzyme with 2-cyclohexenone (*18*). While the other kinetic constants obtained from this analysis (Table 1) are similar to those of the OYE's (*26*), substrate inhibition has not been reported for those proteins. It has been observed in other homologs of EBP1 and OYE (*9*, *27*).

Scheme 3

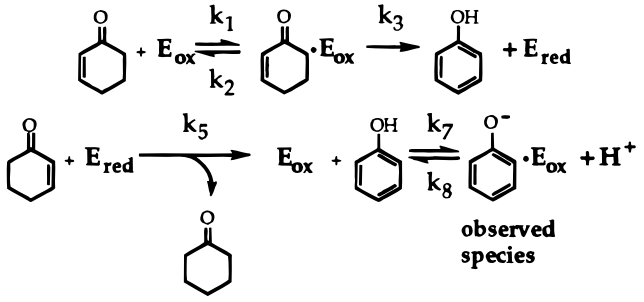

Table 1: Substrate Reactivity Profile for EBP1

compound	$K_{m(app)}$ (μM)	$k_{cat(app)}$ (min^{-1})
2-cyclohexen-1-one[a]	26	710
methyl vinyl ketone	5	340
cis & trans, 4-hexen-3-one[b]	30, 250	230, 100
5-hexen-2-one	NA	no turnover
crotonic acid	NA	no turnover
crotononitrile	NA	no turnover
cinnamaldehyde	15	500
trans-2-hexenal[a]	13	720

[a] True steady-state constants for these compounds were obtained by varying both substrates. For other compounds listed, apparent values were obtained using 20 μM NADPH, $\geq 10K_{mNADPH}$. [b] Values obtained with a mixture of both isomers; thus, particular constants cannot be assigned to either.

With the significant substrate inhibition by 2-cyclohexenone, further characterization of inhibition by estradiol using this substrate would be difficult. Therefore, we evaluated a number of other α,β-unsaturated carbonyl compounds as potential substrates. As with OYE, a variety of compounds with an α,β-unsaturated keto or aldehyde function, as well as O_2, serve as electron acceptors in the EBP1-catalyzed oxidation of NADPH (Table 1). (The oxidase rate at 20% O_2, 20 μM NADPH is about 30 min^{-1}.) *trans*-2-Hexenal exhibited both a high turnover rate ($k_{cat} = 720 \pm 20$ min^{-1}) and a relatively low Michaelis constant ($K_m = 13 \pm 1$ μM), properties favorable for studying the kinetic mechanism of this redox reaction and its inhibition. As shown in Figure 5, double-reciprocal plots of the velocity dependence on varying concentrations of NADPH and hexenal yield a family of parallel lines, indicating a tetra uni ping pong mechanism like the reaction with 2-cyclohexenone at noninhibitory

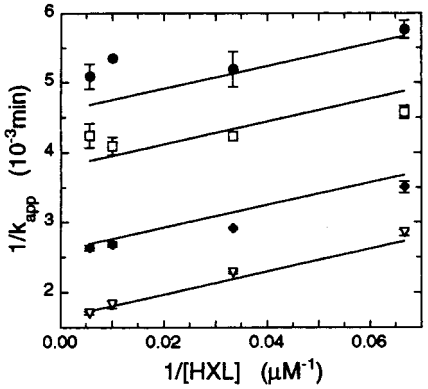

FIGURE 5: Double-reciprocal plot of steady-state velocity data using NADPH and *trans*-2-hexenal as substrates: (—●—) 0.75 μM, (—□—) 1 μM, (—◆—) 2 μM, and (—▽—) 10 μM NADPH. Data analysis as described in text yields $K_{mNADPH} = 1.7 \pm 0.1$ μM, $K_{mHXL} = 13 \pm 1$ μM, and $k_{cat} = 720 \pm 20$ min^{-1}.

concentrations. The slight deviation from the expected velocity in this case when both NADPH concentration is low and hexenal concentration is high suggests only very weak binding of the unsaturated aldehyde to the oxidized enzyme, a feature shared with the other acyclic compounds tested. Thus, we have chosen *trans*-2-hexenal for our standard assays to evaluate inhibition by steroids. Like OYE and OPDA reductase (*28*, *29*), EBP1 prefers NADPH over NADH, with a rate of turnover $\geq$40-fold higher using NADPH as the source of electrons (data not shown).

Steroid Inhibition of Steady-State Turnover. The inhibition behavior of estradiol was determined by systematically varying the concentration of estradiol and one substrate with a constant, saturating concentration of the other. Double-reciprocal plots of velocity data thus obtained are shown in Figure 6. Although the data are more scattered at high concentrations of estradiol, the convergence at the $1/k_{app}$ axis indicates that this steroid binds competitively with NADPH (Figure 6A). Furthermore, because of the complementarity in a ping pong system, a compound which acts purely competitively with respect to one substrate must be uncompetitive with respect to the other. Indeed, as shown in Figure 6B, estradiol binds uncompetitively with respect to the oxidizing substrate, *trans*-2-hexenal, resulting in a family of parallel lines with varied inhibitor concentrations. The simplest interpretation of these data is that the only significant interaction of estradiol is with the oxidized form of the enzyme, and the inhibition constant obtained from analysis of both sets of data, $K_i = 10 \pm 2$ nM, represents a dissociation constant for the E_{ox}•estradiol complex. This agrees well with a dissociation constant of 6.2 nM determined previously using an equilibrium binding assay (*6*).

Since many α,β-unsaturated ketones are substrates for this enzyme, we were interested in whether a steroid with such a structure might bind and inhibit the NADPH−hexenal redox reaction, or serve as an additional substrate. 19-Nortestosterone shares the cyclopentanophenanthrene structure with estradiol, but the A ring contains an α,β-unsaturated ketone instead of the phenolic ring of estradiol (see Figure 8B, inset). In contrast to the results for estradiol, double-reciprocal plots generated by systematically varying nortestosterone and each substrate in the presence of saturating concentrations of the second substrate reveal families of lines that intersect slightly to the left of the $1/k_{app}$ axis (Figure

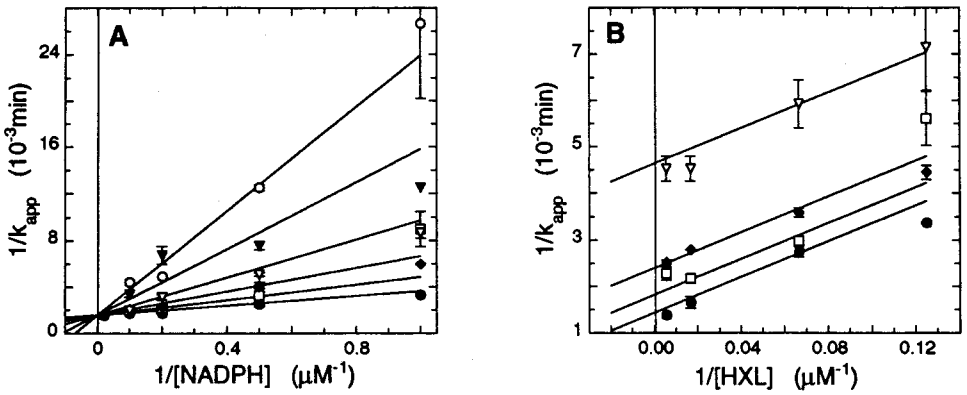

FIGURE 6: Inhibition of steady-state turnover by estradiol. (A) Inhibition with respect to NADPH. Saturating HXL (180 μM) (13$K_{m,HXL}$) was used while varying [NADPH] and [estradiol]: (—●—) 0, (—□—) 6 nM, (—◆—) 15 nM, (—▽—) 30 nM, (—▼—) 60 nM, and (—○—) 100 nM estradiol in assay. (B) Inhibition with respect to HXL. Saturating NADPH (30 μM) (15$K_{m,NADPH}$) was used while varying [HXL] and [estradiol]: (—●—) 0, (—□—) 60 nM, (—◆—) 150 nM, and (—▽—) 500 nM estradiol in assay. Curves in (A) and (B) were generated from a global least-squares fit to the data, as described, with $K_i = 10 \pm 2$ nM, the dissociation constant for E_{ox}·estradiol complex.

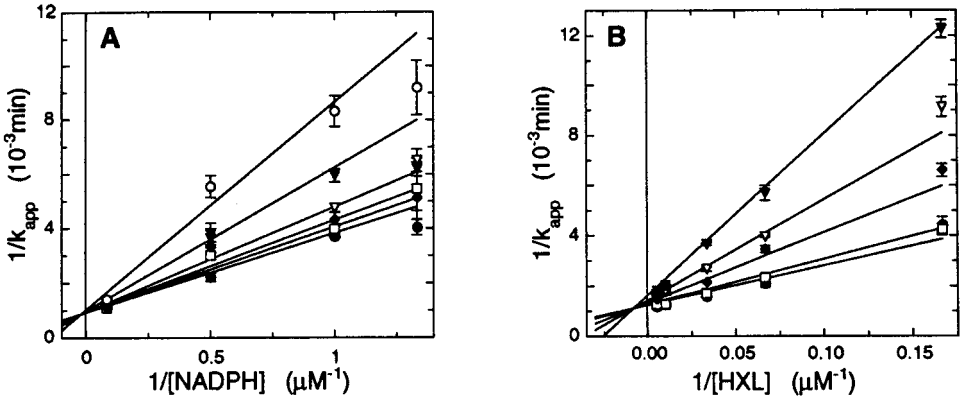

FIGURE 7: Inhibition of steady-state turnover by 19-nortestosterone. (A) Inhibition with respect to NADPH. Saturating HXL (180 μM) (13$K_{m,HXL}$) was used while varying [NADPH] and [19-nortestosterone]: (—●—) 0, (—□—) 50 nM, (—◆—) 100 nM, (—▽—) 200 nM, (—▼—) 500 nM, and (—○—) 1 μM 19-nortestosterone in assay. (B) Inhibition with respect to HXL. Saturating NADPH (30 μM) (15$K_{m,NADPH}$) was used while varying [HXL] and [19-nortestosterone]: (—●—) 0, (—□—) 100 nM, (—◆—) 500 nM, (—▽—) 1 μM, and (—▼—) 2 μM 19-nortestosterone in assay. Curves in (A) and (B) were generated from a global least-squares fit to the data, as described, with $K_i = 600 \pm 100$ nM, the dissociation constant for the E_{ox}·19-nortestosterone complex, and $K_i' = 650 \pm 90$ nM, the dissociation constant for the E_{red}·19-nortestosterone complex.

7A,B). In this case, the inhibition appears to be mixed, that is, the inhibitor binds to both the oxidized and the reduced forms of the enzyme. The dissociation constants for binding to E_{ox} and E_{red} obtained from analysis of the data according to eq 4 are 600 ± 100 and 650 ± 90 nM, respectively. It is interesting to note that both cyclic enones tested here, cyclohexenone and nortestosterone, behaved in this fashion, that is, bound to both forms of the enzyme. This is of particular interest in light of the fact that the substrate of the homolog OPDA reductase is indeed a cyclic enone. Perhaps the ability to bind both forms of the enzyme serves a biological purpose, for example, a regulatory role.

Disproportionation of Cyclic α,β-Unsaturated Ketones. To further characterize the interaction of EBP1 with the cyclic compound cyclohexenone, we examined the changes in the UV−vis spectrum that occur upon mixing under anaerobiosis. It has been shown previously that addition of 2-cyclohexenone to oxidized OYE results in the time-dependent development of a species with a spectrum identical to that of the E_{ox}·phenoxide complex. This observation led to the discovery that phenol is generated by the enzyme under these conditions via aromatization of the cyclic α,β-unsaturated ketone (*26*). In the absence of O_2 or another electron acceptor, two moles of cyclohexenone are disproportionated to give one mole of phenol and one mole of cyclohexanone. As shown in Figure 8A, anaerobic addition of 2-cyclohexenone to oxidized EBP1 results in an immediate spectral change characterized by a broad, low-intensity, long-wavelength absorbance followed by the slow conversion to a species with long-wavelength absorbance similar to that resulting from direct addition of phenol to the enzyme (cf. Figure 1). This suggests that EBP1 also facilitates the oxidation and concomitant aromatization of 2-cyclohexenone, as well as its reduction. Retention times of the recovered products of the reaction analyzed by RP-HPLC are identical to those for standards of cyclohexanone and phenol (data not shown).

The appearance of the long-wavelength absorbance in Figure 8A displays complex kinetic behavior, as was also noted in the analogous reaction of OYE with 2-cyclohexenone (*26*). The complexity can be explained by the reactions summarized in Scheme 3. Rapid formation of the initial E_{ox}·cyclohexenone complex results in an immediate small increase in the long-wavelength absorbance, possibly due to charge transfer from an enolate form of the bound cyclohexenone. Further development of the more intense charge-transfer absorbance, which is used to monitor the kinetics, results from formation of the E_{ox}·phenoxide com-

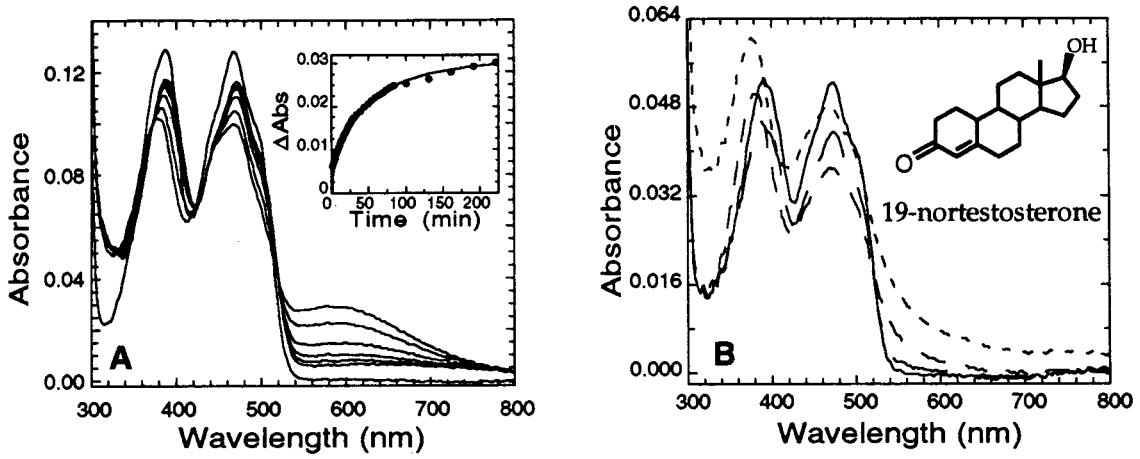

FIGURE 8: Dismutation of cyclic enones by EBP1. (A) 2-cyclohexenone (final concentration of 600 μM) was tipped into an anaerobic solution of oxidized enzyme (11 μM) in 0.1 M phosphate buffer, pH 7.2, at 25 °C. Spectra with increasing long-wavelength absorbance were collected at 0, 1, 4.5, 9, 21, 61.5, and 176.5 min after addition. Inset: Increase in absorbance at 578 nm as a function of time. The solid curve represents a fit to the data using the model described in Scheme 3. (B) 19-nortestosterone (final concentration of 13 μM) was tipped into an anaerobic solution of oxidized enzyme (6.5 μM) in 0.1 M phosphate buffer, pH 7.2, at 25 °C. Spectra were collected at (—) 2, (— — —) 62, (- - -) 602, and (•••) 2490 min after addition.

plex. However, as summarized in Scheme 3, this first requires reduction of E_{ox} by cyclohexenone to generate phenol, followed by reoxidation of E_{red} by a second mole of cyclohexenone to regenerate E_{ox}. Phenol then competes with cyclohexenone for E_{ox} to yield the charge-transfer complex. Since formation of the complex removes the enzyme needed to catalyze the formation of the charge-transfer-generating ligand, the kinetics are not expected to follow a single exponential. To estimate the rate constants that comprise this reaction, we attempted to measure the kinetics for binding of 2-cyclohexenone and phenol to E_{ox} using a stopped-flow spectrophotometer. However, all spectral changes were complete in the dead time of the instrument at all concentrations of ligand used, yielding only lower limits for the sum of $k_{on}[L] + k_{off}$ for each ligand (data not shown). By using these lower limit estimates combined with the measured dissociation constants, $K_d = k_{off}/k_{on}$, we were able to constrain a fit to the model in Scheme 3 with at least minimal values for k_1, k_2, k_7, and k_8. In addition, reoxidation of E_{red} by cyclohexenone is rapid even with stoichiometric cyclohexenone (unpublished data); thus, this reaction was modeled as a second-order process since the concentration of E_{red} will be very low throughout the reaction. Combining all this information, a reasonable fit of the experimental data to the model shown in Scheme 3 was obtained (Figure 8A, inset) and yielded estimates for k_5 of 1×10^6 M^{-1} s^{-1} and for k_3 of 0.55 ± 0.05 s^{-1}. If allowed to vary, the rapid binding rates (k_1, k_2, k_7, and k_8) were too high to obtain accurately from the fitting procedure and, thus, were simply constrained as described above.

With the observation that 2-cyclohexenone not only binds to, but also reacts with, both E_{ox} and E_{red}, we next investigated the possibility that the steroid 19-nortestosterone, a substituted cyclic enone, might also react with EBP1 in a similar manner. Unlike titration with ligands containing a phenolic moiety, addition of 19-nortestosterone to oxidized enzyme does not result in immediate formation of a new, discrete long-wavelength absorbance (Figure 8B, first curve). Instead, the major flavin bands are shifted initially to slightly longer wavelength and have somewhat smaller extinction coefficients. Analysis of the absorbance changes as a function of added ligand shows that binding is quite tight, precluding measurement of a K_d by this method. After aerobic incubation of the enzyme with this steroid overnight, the main flavin absorption bands shift back to shorter wavelength, as in the spectrum of the E_{ox}•estradiol complex, suggesting that the starting material is aromatized (data not shown). During anaerobic incubation, the initial complex converts to a species with partially reduced flavin (Figure 8B, medium dashed line), and this is followed by the apparent reoxidation of the flavin in an unusual manner (Figure 8B, dotted line). This process is quite slow, and displays complex kinetics, as in the disproportionation of 2-cyclohexenone. High-resolution mass spectrometry of the products recovered after incubation revealed formation of two products, with masses of 272.2 and 276.2, corresponding to the oxidized and reduced products, estradiol and estran-17β-ol-3-one, consistent with the proposed dismutation of 19-nortestosterone by EBP1.

The character of the flavin spectrum during the reoxidation by this steroid suggests that one electron-reduced, anionic flavin semiquinone is partially stabilized under these conditions. To examine this in more detail, we examined the half-reaction of reduced enzyme with nortestosterone. Anaerobic addition of a substoichiometric quantity (~0.9 equivalents) of 19-nortestosterone to enzyme reduced with sodium dithionite resulted in an immediate change in the UV—vis absorption spectrum and the slow reoxidation of the flavin (Figure 9). Indeed, until the end of the reaction, and unlike the reoxidation of E_{red} by either 2-hexenal or 2-cyclohexenone (data not shown), the flavin absorption spectrum exhibits some of the anionic red semiquinone character seen with OYE under certain conditions (*22*). This intermediate also appears transiently upon anaerobic reduction of EBP1 with the one-electron donor, sodium dithionite, but is not stable in the absence of steroid. Mass spectrometric data confirmed that the product recovered from the reaction after opening to air has a mass of 276.2 Da, as expected for the product of 19-nortestosterone in which the 4,5 double bond has been reduced, estran-17β-ol-3-one.

In conclusion, EBP1 has been shown to be capable of the dismutation of both cyclic enones tested here. This feature

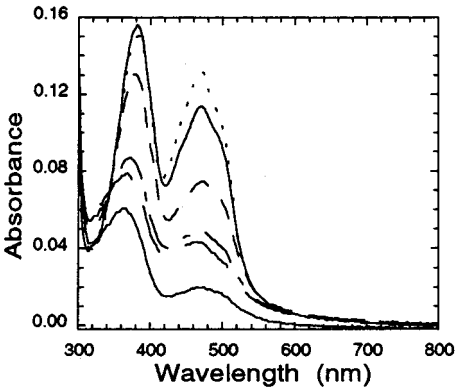

FIGURE 9: Anaerobic reoxidation of reduced EBP1 by 19-nortestosterone. Slightly less than one equivalent of 19-nortestosterone was tipped into an anaerobic solution of enzyme (12 μM), previously reduced stoichiometrically with dithionite in 0.1 M phosphate buffer, pH 7.2, at 25 °C. Spectra were collected at (lower solid) 0, (− − −) 1, (− - −) 19, (- - -) 181, (upper solid) 781, and (···) 2461 min after addition.

was perhaps hinted at both in the substrate inhibition by 2-cyclohexenone and in the demonstration in the inhibition study of the ability for the oxidized and reduced forms of the enzyme to bind 19-nortestosterone. While the redox turnover of this steroid no doubt complicates the full kinetic scheme describing its interaction with the enzyme during turnover of NADPH and hexenal, turnover of the steroid is so much slower than that of the other compounds that it is insignificant and can be ignored in the determination of the inhibition constants.

DISCUSSION

The steady-state inhibition and spectral titration data presented here indicate for the first time that EBP1 binds estradiol, phenol, and nortestosterone in its active site, and imply a mechanism by which these compounds inhibit the NADPH-oxidase activity of this enzyme. This study has also revealed the extensive similarity between the properties of EBP1 and those of its OYE homologs, as well as some differences. Despite extensive conservation of residues that, on the basis of the crystal structure of OYE (*30*), appear in the active site of the enzyme, our results suggest that the electronic environments in the two proteins are slightly different. This is evident in the difference between the two-electron reduction potential of the flavin on the two enzymes. Another indication that the proteins stabilize the redox states of cofactor differentially is their very different behavior upon reduction with electron donors that transfer single-electron equivalents. Stewart and Massey (*22*) reported that the one-electron-reduced FMN form of OYE can be generated nearly quantitatively upon reductive titration of that protein with the single-electron donor, sodium dithionite. In contrast, similar titrations of EBP1 result in only transient formation of this species, which then rapidly disproportionates to the fully oxidized and two-electron-reduced forms, indicating that the midpoint potential of the $E_{ox} + e^- \leftrightarrow E_{sq}^{\bullet}$ couple is significantly lower in EBP1 relative to the $E_{ox} + 2e^- \leftrightarrow E_{red}$ couple than it is in the OYE system.

Another difference between these two proteins is the extent to which the pK_a of the phenolic ligand is lowered in the active site. Results here show that the phenolic pK_a's are lowered ~3 pH units by EBP1, but similar results presented for OYE indicate a shift of ≥4 pH units, an order of magnitude greater stabilization of the anion than in EBP1 (*23*, *25*). Stabilization of the anion of phenolic ligands could be relevant to catalysis, if these compounds represent analogues of the physiological oxidizing substrates of the proteins. The powerful electronic effect exerted on the phenol results in the stabilization of the phenoxide anion by 3 orders of magnitude, corresponding to a $\Delta\Delta G = -4.2$ kcal/mol, relative to that in solution. This same force acting on the carbonyl oxygen of the substrate could be used to polarize the conjugated enone to drive its reduction at C3, i.e., electrophilic catalysis. The differences between the proteins shown here in the redox potentials of their cofactors and the electronic effect exerted on their ligands may be a reflection of the fact that they come from different organisms and act upon different substrates that, while structurally similar, have different electronic properties. Alternatively, the proteins might act on the same or very similar substrates, and the implicit stronger anion stabilization by OYE indicated by the lower pK_a of phenol in the OYE active site, and thus ability to polarize the appropriate carbonyl bond of an α,β-unsaturated substrate versus EBP1, may have evolved to compensate for the higher redox potential of its FMN cofactor relative to that of EBP1.

As illustrated in Table 1, EBP1 is not very discriminating with respect to the electron acceptor in the reaction with NADPH. In general, compounds with an α,β-unsaturated ketone or aldehyde structure serve well as electron acceptors. The results with those compounds tested parallels reactivity seen in the OYE system, with k_{cat} values similar to those reported for both OYE2 and OYE3 (*8*). Though the products of some of these reactions were not identified explicitly, it is likely that the flavin is reoxidized as in the reaction of reduced enzyme with 2-cyclohexenone, with transfer of hydride from the reduced flavin to the olefinic bond of the substrate. Furthermore, as with OYE, the α,β-unsaturated acid and nitrile were not able to stimulate oxidation of NADPH by EBP1, probably the result of an inability of the enzyme to position these compounds properly for the reduction and/or an electronic effect, that is, a decreased ability of the functional group to pull electron density from the carbon−carbon double bond and thus help drive hydride transfer. The ability of EBP1 to catalyze reduction of OPDA or similar lipids has not yet been investigated, but the reactivity with these other compounds, particularly the lipophilic 19-nortestosterone, strongly suggests it will be able to do so. It has already been shown that OYE does catalyze such a reaction (*12*).

Perhaps the most significant difference of EBP1 from the OYE's is its reactivity with 19-nortestosterone. Although OYE has been shown to oxidize this steroid, producing estradiol, it is not capable of reducing its carbon−carbon double bond. The same is true of other homologs of EBP1, morphinone reductase and OPDA reductase, which catalyze the reduction of 2-cyclohexenone, but do not reduce steroid substrates (*9*, *12*). In contrast, we found that EBP1 not only oxidizes 19-nortestosterone, but also reduces it, and will disproportionate the steroid if incubated with it anaerobically. It was proposed (*26*) that the inability of OYE to catalyze this reaction arises from steric constraints: the architecture of the active site will only allow the steroid to be positioned such that the 1,2 bond is above N5 of the

isoalloxazine ring, permitting transfer of hydride from the steroid to the flavin, resulting in oxidation and aromatization to estradiol. Reduction of the compound would require the 4,5 double bond to be oriented above N5 of the reduced flavin for hydride transfer to occur, and Massey and co-workers (*26*) have pointed out that the enzyme would have to be able to bind either face of the steroid molecule to align it in this manner. Either EBP1 is able to do this, or it binds only one face of 19-nortestosterone, which can then move coplanar with the flavin, to position either the 1,2 bond over N5 in oxidized enzyme or the 4,5 bond over N5 in reduced enzyme. The answer to this question awaits solution of the crystal structure of EBP1 and its complexes, which is in progress.

Another interesting feature of the reduction of nortestosterone is the development of intermediate spectra in which it appears that one-electron-reduced anionic semiquinone is formed during the course of the reaction. This could indicate that the reduction of 19-nortestosterone proceeds with the stepwise transfer of single electrons and the formation of a radical pair consisting of the one-electron reduced steroid and flavin. If this is the case, the results imply that the transfer of the first electron to the steroid is significantly faster than the second, so that the radical pair is kinetically stable. Another possibility is that reduction of the steroid occurs via a rapid two-electron transfer of hydride to the steroid, followed by comproportionation of two enzyme molecules, one fully reduced and the other fully oxidized, to give two equivalent one-electron-reduced species. As mentioned above, this is not a stable species of EBP1 when no steroid is present, so it seems, regardless of which mechanism is correct, that some component(s) of the steroid reactant, product, or possibly a one-electron-reduced intermediate stabilizes the FMN semiquinone in the active site. Further studies to fully characterize this reaction and the relevant species are being pursued.

The estrogen-binding protein has been shown here to exhibit a much more diverse array of functions than its name suggests, and identifies it functionally as a member of the OYE family of enzymes. Indeed, the estrogen- and phenol-binding activity may be just a fortuitous consequence of the biological role this enzyme plays. It has been reported that *C. albicans* responds to exogenous estrogens with changes in growth rate and morphology, and that the hormonal environment of the human host could, therefore, contribute to its pathogenicity. Since EBP1 is the major, if not exclusive, protein in this organism that binds estrogens (*6*), perhaps it mediates this response. It is possible that EBP1 functions in a pathway analogous to the octadecanoid pathway of its plant homolog, OPDA reductase, and that it is responsible for the generation of a signaling molecule within *C. albicans*. In this case, it could be that inhibition of this enzyme by estrogens and the subsequent buildup of some precursor(s) result in the observed changes. Experiments are underway to examine this potential relationship between EBP1 and *C. albicans* morphology and virulence.

ACKNOWLEDGMENT

We are grateful for the generous gift of the pMAL-EBP1 plasmid and *C. albicans* strain 422 from Drs. Peter Malloy and David Feldman (Stanford).

REFERENCES

1. Kinsman, O. S., and Collard, A. E. (1986) *Infect. Immun. 53*, 498−504.
2. Kinsman, O. S., Pitblado, K., and Coulson, C. J. (1988) *Mycoses 31*, 617−626.
3. Gujjar, P. R., Finucane, M., and Larsen, B. (1997) *Ann. Clin. Lab. Sci. 27*, 151−156.
4. Odds, F. C. (1988) *Candida and candidosis*, 2nd ed., Bailliere Tindall, Philadelphia, PA.
5. Powell, B. L., Frey, C. L., and Drutz, D. J. (1984) *Exp. Mycol. 8*, 304−313.
6. Madani, N., Malloy, P., Rodriguez-Pombo, P., Krishnan, A., and Feldman, D. (1994) *Proc. Natl. Acad. Sci. U.S.A. 91*, 922−926.
7. Warburg, O., and Christian, W. (1932) *Naturwissenshaften 20*, 688.
8. Niino, Y. S., Chakraborty, S., Brown, B. J., and Massey, V. (1995) *J. Biol. Chem. 270*, 1983−1991.
9. French, C. E., and Bruce, N. C. (1994) *Biochem. J. 301*, 97−103.
10. Franklund, C. V., Baron, S. F., and Hylemon, P. B. (1993) *J. Bacteriol. 175*, 3002−3012.
11. Miura, K., Tomioka, Y., Suzuki, H., Yonezawa, M., Hishinuma, T., and Mizugaki, M. (1997) *Biol. Pharm. Bull. 20*, 110−112.
12. Schaller, F., and Weiler, E. W. (1997) *J. Biol. Chem. 272*, 28066−28072.
13. Abramovitz, A. S., and Massey, V. (1976) *J. Biol. Chem. 251*, 5321−5326.
14. Buckman, J., Miller, S. M., Malloy, P., and Feldman, D. (1996) in *Flavins and Flavoproteins 1996*: *Twelfth International Symposium* (Stevenson, K. J., Massey, V., and Williams, C. H., Jr., Eds.) pp 81, University of Calgary Press, Calgary, Alberta, Canada.
15. Sambrook, J., Fritsch, E., and Maniatis, T. (1989) *Molecular Cloning*: *A Laboratory Manual*, 2nd ed., Cold Spring Harbor Laboratory Press, Plainview, NY.
16. Ellis, K. J., and Morrison, J. F. (1982) *Methods Enzymol. 87*, 405−426.
17. Dixon, M. (1953) *Biochem. J. 55*, 161−170.
18. Segel, I. H. (1975) *Enzyme kinetics*: *Behavior and analysis of rapid equilibrium and steady-state enzyme systems*, John Wiley and Sons, New York.
19. Williams, C. H., Jr., Arscott, L. D., Matthews, R. G., Thorpe, C., and Wilkinson, K. D. (1979) *Methods Enzymol. 62*, 185−98.
20. Fultz, M. L., and Durst, R. A. (1982) *Anal. Chim. Acta 140*, 1−18.
21. Matthews, R. G., Massey, V., and Sweeley, C. (1975) *J. Biol. Chem. 250*, 9294−8298.
22. Stewart, R. C., and Massey, V. (1985) *J. Biol. Chem. 260*, 13639−13647.
23. Abramovitz, A. S., and Massey, V. (1976) *J. Biol. Chem. 251*, 5327−5336.
24. Dawson, R. M. C., Elliot, D. C., Elliot, W. H., and Jones, K. M. (1969) *Data for Biochemical Research*, 2nd ed., Clarendon Press, New York.
25. Massey, V. (1993) in *Flavins and Flavoproteins 1993*: *Eleventh International Symposium* (Yagi, K., Ed.) pp 371−380, Walter de Gruyter, Nagoya, Japan.
26. Vaz, A. D. N., Chakraborty, S., and Massey, V. (1995) *Biochemistry 34*, 4246−4256.
27. French, C. E., Nicklin, S., and Bruce, N. C. (1996) *J. Bacteriol. 178*, 6623−6627.
28. Brown, B. J., and Massey, V. (1996) in *Flavins and Flavoproteins 1996*: *Proceedings of the Twelfth International Symposium* (Stevenson, K. J., Massey, V., and Williams, C. H., Jr., Eds.) pp 77−80, University of Calgary Press, Calgary, Alberta, Canada.
29. Schaller, F., and Weiler, E. W. (1997) *Eur. J. Biochem. 245*, 294−299.
30. Fox, K. M., and Karplus, P. A. (1995) *Structure 2*, 1089−1105.

BI981106Y